ACCOUNTS
of chemical research

Surface-Modified Silica Colloidal Crystals: Nanoporous Films and Membranes with Controlled Ionic and Molecular Transport

ILYA ZHAROV* AND AMIR KHABIBULLIN

Department of Chemistry, University of Utah, Salt Lake City, Utah 84112, United States

RECEIVED ON JUNE 30, 2013

CONSPECTUS

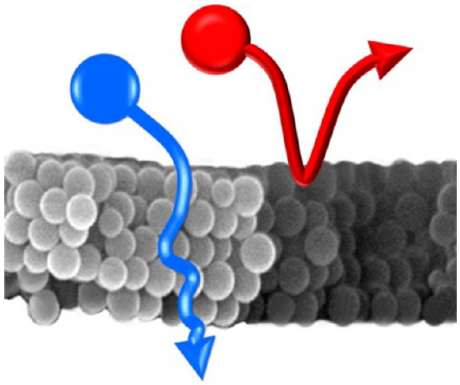

Nanoporous membranes are important for the study of the transport of small molecules and macromolecules through confined spaces and in applications ranging from separation of biomacromolecules and pharmaceuticals to sensing and controlled release of drugs. For many of these applications, chemists need to gate the ionic and molecular flux through the nanopores, which in turn depends on the ability to control the nanopore geometry and surface chemistry. Most commonly used nanoporous membrane materials are based on polymers. However, the nanostructure of polymeric membranes is not well-defined, and their surface is hard to modify. Inorganic nanoporous materials are attractive alternatives for polymers in the preparation of nanoporous membranes.

In this Account, we describe the preparation and surface modification of inorganic nanoporous films and membranes self-assembled from silica colloidal spheres. These spheres form colloidal crystals with close-packed face centered cubic lattices upon vertical deposition from colloidal solutions. Silica colloidal crystals contain ordered arrays of interconnected three dimensional voids, which function as nanopores. We can prepare silica colloidal crystals as supported thin films on various flat solid surfaces or obtain free-standing silica colloidal membranes by sintering the colloidal crystals above 1000 °C. Unmodified silica colloidal membranes are capable of size-selective separation of macromolecules, and we can surface-modify them in a well-defined and controlled manner with small molecules and polymers. For the surface modification with small molecules, we use silanol chemistry. We grow polymer brushes with narrow molecular weight distribution and controlled length on the colloidal nanopore surface using atom transfer radical polymerization or ring-opening polymerization.

We can control the flux in the resulting surface-modified nanoporous films and membranes by pH and ionic strength, temperature, light, and small molecule binding. When we modify the surface of the colloidal nanopores with ionizable moieties, they can generate an electric field inside the nanopores, which repels ions of the same charge and attracts ions of the opposite charge. This allows us to electrostatically gate the ionic flux through colloidal nanopores, controlled by pH and ionic strength of the solution when surface amines or sulfonic acids are present or by irradiation with light in the case of surface spiropyran moieties. When we modify the surface of the colloidal nanopores with chiral moieties capable of stereoselective binding of enantiomers, we generate colloidal films with chiral permselectivity. By filling the colloidal nanopores with polymer brushes attached to the pore surface, we can control the ionic flux through the corresponding films and membranes electrostatically using reversibly ionizable polymer brushes. By filling the colloidal nanopores with polymer brushes whose conformation reversibly changes in response to pH, ionic strength, temperature, or small molecule binding, we can control the molecular flux sterically.

There are various potential applications for surface-modified silica colloidal films and membranes. Due to their ordered nanoporous structure and mechanical durability, they are beneficial in nanofluidics, nanofiltration, separations, and fuel cells and as catalyst supports. Reversible gating of flux by external stimuli may be useful in drug release, in size-, charge-, and structure-selective separations, and in microfluidic and sensing devices.

Published on the Web 01/07/2014 www.pubs.acs.org/accounts
10.1021/ar400157w

Introduction

Nanoporous membranes have been used for studying the transport of small molecules and macromolecules through nanopores[1,2] and in various applications, including separation of biomacromolecules[3] and pharmaceuticals,[4] sensing,[5] and novel medical devices.[6−8] Many of these applications are based on gating the nanopore flux by noncovalent interactions of surface-immobilized moieties with the diffusing species[9] or by using responsive polymer molecules that can sterically block and unblock the pores.[10,11]

Inorganic nanoporous materials, both intrinsically porous, such as zeolites,[12] and prepared through nanofabrication (e.g., in silicon nitride[13]), etching (porous silicon[14] and anodized alumina[15]), templating (mesoporous silica[16]), and controlled growth (nanotubes[17]), are attractive alternatives for polymeric membranes.[18] Despite the impressive advances in the field of inorganic nanoporous membrane materials, several problems remain unsolved. Many of the inorganic nanoporous membranes possess low pore density. Second, it is difficult to vary the pore size in a broad range in these materials. In addition, many of these membranes require specialized methods for their preparation. In contrast, silica colloidal membranes, developed in our group in the past several years, provide a simple and powerful approach to self-assembled nanoporous membranes with high ionic and molecular flux, nanopore size that can be easily varied in the 5−50 nm range, and facile surface chemistry that allows gating of ionic and molecular flux using a variety of external stimuli.

Originally, silica colloidal crystals were developed as templates for the preparation of photonic[19] and magnetic materials,[20] macroporous polymer membranes,[21] and sensors.[22] Silica colloidal crystals consist of a close-packed face-centered cubic (fcc) lattice of silica spheres of a submicrometer diameter (Figure 1) with ordered arrays of interconnected three-dimensional nanoscale voids, which constitute the nanopores.[23] The synthesis of silica spheres is simple,[24] preparation of colloidal crystals by self-assembly of the spheres is well developed,[25] and void size in the crystals can be readily varied by the sphere size. Because of the three-dimensional geometry of the voids, we use their projection (Figure 1A) as a simplified description of the pore geometry. The distance between the center of this projection and the silica sphere surface, which we call the nanopore "radius", is ca. 15% of the silica sphere radius.

The surface silanol groups in colloidal crystals can be modified by nucleophilic silylation to introduce a variety of

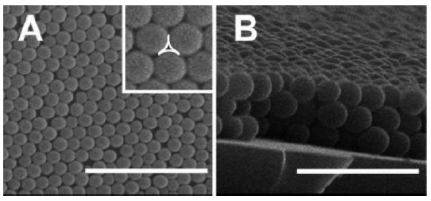

FIGURE 1. SEM images of silica colloidal films prepared on glass from 440 nm diameter silica spheres deposited (A) top view (scale bar 4 μm) and (B) side view (scale bar 2 μm). The geometric projection of a pore observed from the (111) plane is outlined in the inset in panel A. Reproduced with permission from ref 31. Copyright 2005 American Chemical Society.

functional groups.[26] Alternatively, the silica surface can be modified with 3-aminopropyltriethoxysilane, followed by treatment with organic molecules carrying electrophilic moieties, including 2-bromoisobutyryl bromide, which can serve as atom transfer radical polymerization (ATRP) initiator,[27] providing the possibility of growing polymer brushes on the silica surface.

An estimate of the molecular flux, J_{fcc}, in the fcc lattice can be obtained using eq 1:[28]

$$J_{colloid} = (\Delta C/L)(\varepsilon/\tau)D_{sol} \quad (1)$$

where D_{sol} is the diffusivity of molecules in free solution, the void fraction ε (0.26) and the tortuosity τ ($\sim$3.0) are intrinsic geometrical parameters independent of the size of the silica spheres used to prepare the colloidal crystal, ΔC is the concentration gradient, and L is the thickness of the lattice. Based on eq 1, the flux of small molecules diffusing through the (111) plane of a colloidal crystal is only 11.5 times lower compared with its free solution value. Importantly, this flux is independent of the interstitial void size and thus remains significant even in the nanoscale regime, where ionic and molecular flux gating is possible.

The above properties of silica colloidal crystals attracted our attention in terms of using them as highly ordered nanoporous materials. Starting in 2005, we developed a new type of hybrid material, surface-modified colloidal crystals, with gated ionic and molecular flux. These materials are described below.

Colloidal Films Modified with Ionizable Groups

Initially, we focused on supported silica colloidal films. Such films can be assembled on a hydrophilic solid support (glass, oxidized silicon, etc.) using the vertical deposition technique.[29] Because films are placed on a solid support, we used cyclic

voltammetry to study the transport through the colloidal nanopores. Thus, silica colloidal films were deposited onto platinum microelectrodes shrouded in glass (called below *opal electrodes*). We used opal electrodes in voltammetric experiments to demonstrate the nanopore gating by measuring the flux of redox-active species through the nanopores as a function of nanopore surface properties and external conditions.[30]

Aminated and Sulfonated Colloidal Films[31−33]**.** To prepare silica colloidal nanopores with pH- and ionic strength-dependent gating based on electrostatic interactions with charged permeants, we modified the colloidal nanopore surfaces with amino[31,32] and sulfonic[33] groups. We found that the limiting current, i_{lim}, of $Ru(NH_3)_6^{3+}$, was greatly reduced for amine-modified opal electrodes at low pH (Figure 2A) compared with unmodified electrodes. At the same time, i_{lim} for $Fe(CN)_6^{4-}$ and $Fc(CH_2OH)_2$ remained approximately the same before and after the surface amination (Figure 2B). Sulfonation of the colloidal films led to reduced i_{lim} for $IrCl_6^{3-}$ (Figure 3A), increased i_{lim} for $Ru(NH_3)_6^{3+}$ (Figure 3B), and unchanged i_{lim} for $Fc(CH_2OH)_2$ (Figure 3C). These observations are consistent with electrostatic gating of the cationic species by the positively charged nanopores carrying protonated amines on their surface, electrostatic gating of anionic species by the negatively charged nanopores carrying sulfonic groups, and electrostatic attraction of cationic $Ru(NH_3)_6^{3+}$ to the negatively charged sulfonated surface. Our investigations of the effect of pH on the ionic flux through aminated (Figure 2D) and sulfonated (Figure 4) silica colloidal films further confirmed these conclusions. Finally, we found that the flux of $Ru(NH_3)_6^{3+}$ through the sulfonated silica colloidal films decreased with increasing ionic strength (Figure 5A), while increasing ionic strength led to increased flux of $IrCl_6^{3-}$ (Figure 5B), as expected.[33]

The above experiments were conducted at 0.05 M electrolyte concentration, where the Debye screening length (κ^{-1}) is ca. 1.5 nm and the electric field extends ~7.5 nm from the surface (5 κ^{-1}), while the nanopore "radius" was ca. 17 nm. In other words, the electric field blocked only a part of the pore, yet significant electrostatic pore gating was observed. We speculated that this is the result of (i) the

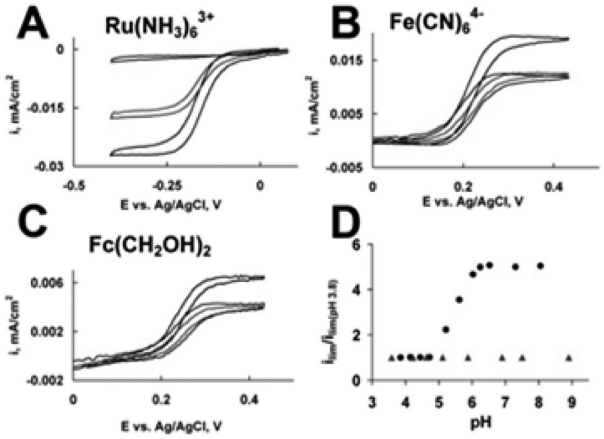

FIGURE 2. Voltammetric responses of a Pt electrode: (A) bare (bottom), after opal assembly (middle), and after chemical modification of the thin colloidal membrane with 3-aminopropyltriethoxysilane (top) at pH 4. (B, C) Bare (top), after opal assembly, and after surface modification of the thin colloidal film with 3-aminopropyltriethoxysilane (middle) at pH 4. (D) Voltammetric responses of as a function of pH for unmodified (triangles) and modified (circles) opal electrode. Reproduced with permission from ref 32. Copyright 2006 American Chemical Society.

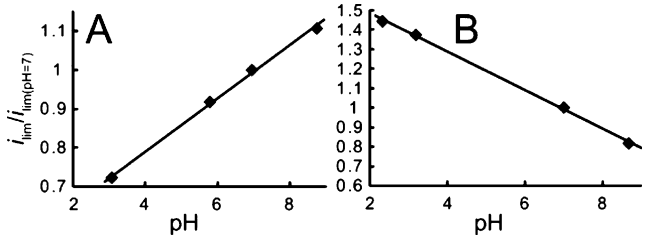

FIGURE 4. Relative limiting current of the sulfonated colloidal membrane electrodes as a function of pH for $Ru(NH_3)_6^{3+}$ (A) and for $IrCl_6^{3-}$ (B). Reproduced with permission from ref 33. Copyright 2008 American Chemical Society.

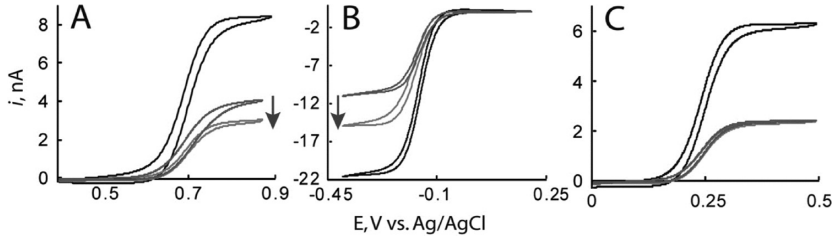

FIGURE 3. Representative voltammetric responses of bare electrodes (top in A and C, bottom in B) and colloidal film electrodes before and after silica surface sulfonation for (A) $IrCl_6^{3-}$ (middle, unmodified film; bottom, sulfonated film), (B) $Ru(NH_3)_6^{3+}$ (top, unmodified film; middle, sulfonated film), and (C) $Fc(CH_2OH)_2$ (middle, unmodified and sulfonated films) at pH 7 with 0.1 M aqueous KCl. The decrease (A) and increase (B) in the limiting current is shown with arrows. Reproduced with permission from ref 33. Copyright 2008 American Chemical Society.

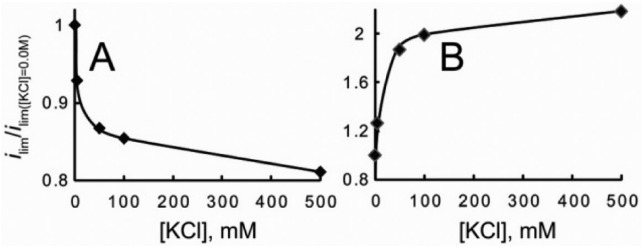

FIGURE 5. Relative limiting current of the sulfonated colloidal membrane electrodes as a function of KCl concentration for $Ru(NH_3)_6^{3+}$ (A) and for $IrCl_6^{3-}$ (B). Reproduced with permission from ref 33. Copyright 2008 American Chemical Society.

tortuosity of the diffusion pathway through the colloidal crystal and (ii) the high surface area of the colloidal crystal.

More recently, we modified the surface of silica colloidal nanopores with spiropyran moieties, which become positively charged upon irradiation with UV light and demonstrated light-responsive ionic gating in the corresponding colloidal films.[34]

Colloidal Films Modified with Chiral Selector Moieties

Once we established that modifying the colloidal nanopores with small ionizable molecules allows gating the ionic flux via noncovalent electrostatic interactions, we became interested in using noncovalent interactions with neutral molecules for controlling their flux. One type of such interaction is stereoselective binding of chiral molecules to surface-immobilized chiral selector moieties (CSMs) through hydrogen bonding and $\pi-\pi$ stacking. Thus, we modified the surface of thin colloidal films with a chiral selector moiety **1** (Chart 1)[35] and studied the flux of three chiral ferrocene derivatives (**2**–**4**, Chart 1) through the resulting chiral colloidal films assembled on Pt microelectrodes shrouded in glass.

We observed the chiral permselectivity by measuring the voltammetric response of **2** for the opal electrodes modified with **1R** (Figure 6A, Table 1). This selectivity was comparable to that reported for chiral antibody-modified nanotube membranes[36] and higher than the selectivity reported for chiral polyelectrolyte membranes.[37] Colloidal films modified with **1S** showed a reversed selectivity (Figure 6B, Table 1). We investigated the transport of two more chiral molecules (**3** and **4**, Chart 1) through the chiral colloidal films and found similar chiral permselectivity that was reversed with the reversal of the surface chirality (Table 1). These results are consistent with a surface facilitated transport mechanism[38] where chiral selectors serve as fixed-site carriers that allow enantiomers to hop from one selector to the next and thus cross the film. Enantiomers interact with the chiral selector moieties to a different extent, which leads to the permselectivity.

CHART 1

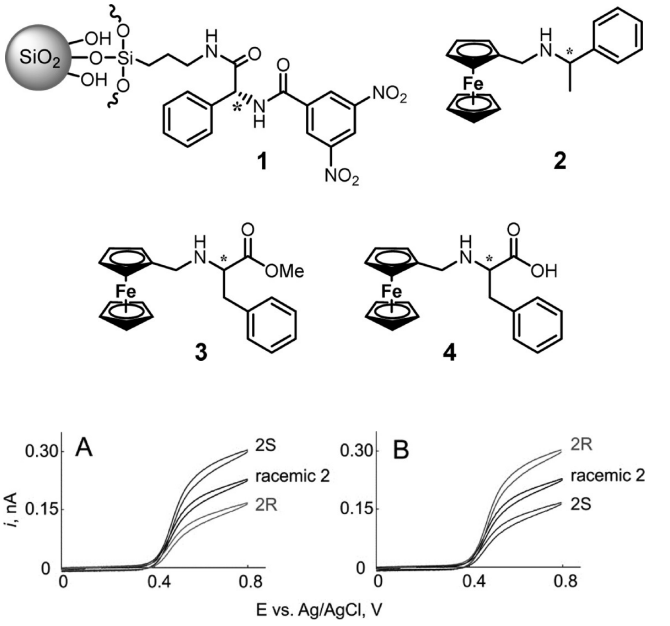

FIGURE 6. (A) Overlay of voltammetric responses of a colloidal film electrode modified with **1R** for **2S** and **2R**. (B) Overlay of voltammetric responses of a colloidal film electrode modified with **1S** for **2S** and **2R**. Adopted with permission from ref 35. Copyright 2006 American Chemical Society.

TABLE 1. Selectivities of the Chiral Colloidal Film Electrode for **2**–**4**

	$i_{lim}(S)/i_{lim}(R)$	
probe	**1R** colloidal film	**1S** colloidal film
2	2.16 ± 0.34	0.58 ± 0.01
3	1.33 ± 0.20	0.82 ± 0.11
4	2.01 ± 0.69	0.84 ± 0.04

We varied the length and structure of the linker attaching the chiral selector moiety **1** to the silica surface and explored the influence of the chiral selector structure (Chart 2) on the permselectivity while maintaining the length of the linker constant (Chart 2).[39] The chiral selectivity of 4.5 found for the chiral selector **7** is one of the highest reported for chiral membranes.

Responsive Polymer-Filled Colloidal Films

After demonstrating that permselectivity in silica colloidal films can be achieved by surface modification with small organic ionizable and supramolecular groups based on noncovalent interactions, our attention turned to sterically gating the molecular flux through the colloidal nanopores using responsive polymers.

CHART 2

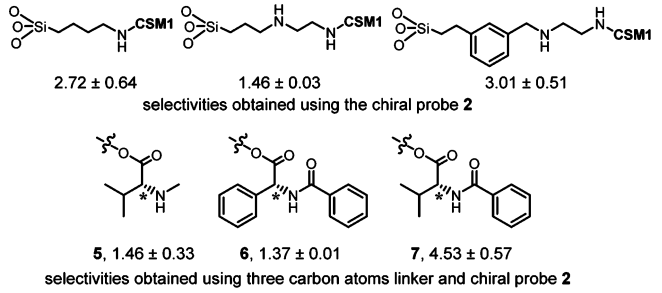

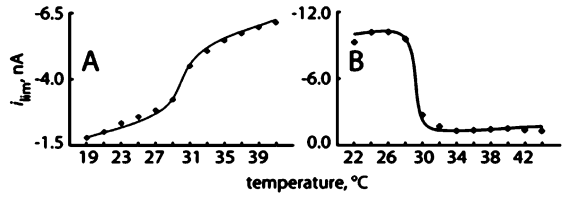

FIGURE 7. Limiting current ($Ru(NH_3)_6^{3+}$) as a function of increasing temperature for PNIPAM−opal film Pt electrodes after polymerization for (A) 15 min and (B) 90 min. Reproduced with permission from ref 40. Copyright 2007 American Chemical Society.

PNIPAM-Filled Colloidal Films[40]. First, we prepared polymer brushes of poly(*N*-isopropylacrylamide), PNIPAM, a well-known temperature responsive polymer,[41] inside the colloidal nanopores using surface-initiated ATRP[42] and measured the temperature response for the membranes modified at different polymerization times. As can be seen in Figure 7, we observed two types of gating. In the case of nanoporous films whose pores were filled with a thin polymer brush, the limiting current increased with temperature (Figure 7A). For colloidal films filled with a thick polymer brush, the limiting current decreased with increasing temperature (Figure 7B). These results suggest that two different of PNIPAM morphologies may form inside the nanopores. At short polymerization time, PNIPAM forms a dense brush (Figure 8A), and the probe molecules diffuse through the polymer-free volume of the nanopores. At higher temperature, the polymer chains collapse, providing a larger free volume for the diffusion (Figure 8A) and increased molecular flux. At longer polymerization time, polymer chains meet and interpenetrate in the middle of the nanopores, leading to a highly porous and permeable hydrogel structure (Figure 8B). At higher temperature, the hydrogel does not shrink to open the nanopores but becomes dehydrated and impermeable (Figure 8B).

Polyalanine-Filled Colloidal Films[43]. We prepared another type of colloidal nanopores gated by a temperature-responsive polymer, those modified with polyalanine.[44] We

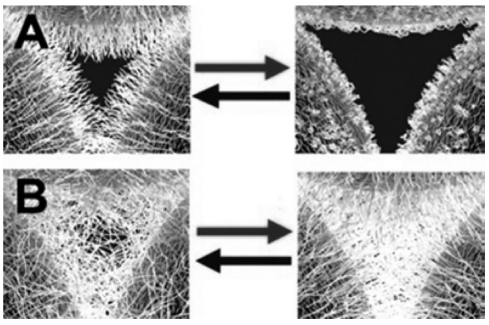

FIGURE 8. Schematic representation of the processes that occur upon heating and cooling of a (A) PNIPAM brush (15 min polymerization) and (B) PNIPAM gel (90 min polymerization) inside a colloidal nanopore. Reproduced with permission from ref 40. Copyright 2007 American Chemical Society.

investigated the temperature response for poly(L-alanine)-filled colloidal films (Scheme 1) using cyclic voltammetry and a neutral probe molecule, $Fc(CH_2OH)_2$. The limiting current for the opal electrodes modified with a poly(L-alanine) brush reversibly increased with increasing temperature (Figure 9). For the colloidal films modified with a thinner polymer brush, the transition temperature was ca. 65 °C (Figure 9A,B), while for the films modified with a thicker polymer brush, the transition temperature was higher, ca. 75 °C (Figure 9C,D).

PDMAEMA-Filled Colloidal Films[45]. Next, we filled the colloidal nanopores with polymer brushes of 2-(dimethylamino)ethyl methacrylate (DMAEMA),[45] whose environmental response is controlled by electrostatic and hydrophobic interactions. We observed a ~80% increase in the flux of $Ru(NH_3)_6^{3+}$ through PDMAEMA-filled colloidal films with increasing pH (Figure 10). The flux increased abruptly at pH ≈ 4−5 (Figure 11), above which the amines in the polymer are deprotonated and thus do not repel the diffusing positively charged $Ru(NH_3)_6^{3+}$. At this pH, the polymer also exists in a collapsed conformation and the diffusion of $Ru(NH_3)_6^{3+}$ is not hindered sterically. On the other hand, at low pH, the polymer chains become protonated and thus stretch. This blocks the diffusion of $Ru(NH_3)_6^{3+}$ both electrostatically and sterically. For comparison, we measured the flux of a neutral redox-active molecule, $Fc(CH_2OH)_2$, through PDMAEMA-filled colloidal films. $Fc(CH_2OH)_2$ limiting current decreased only by ~30% (Figure 10B) at lower pH, which should correspond exclusively the steric hindrance by the PDMAEMA chains.

We found that the diffusion across the protonated PDMAEMA-filled colloidal films was affected by the solution ionic strength. The flux of both $Ru(NH_3)_6^{3+}$ and $Fc(CH_2OH)_2$

SCHEME 1

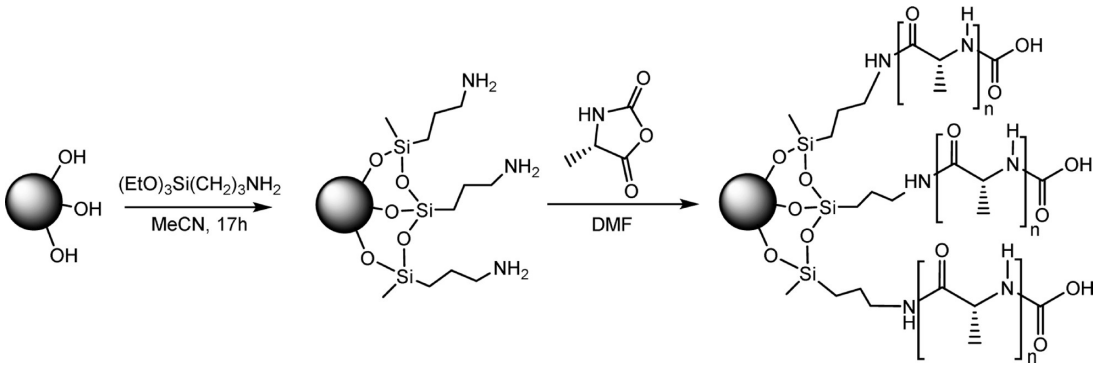

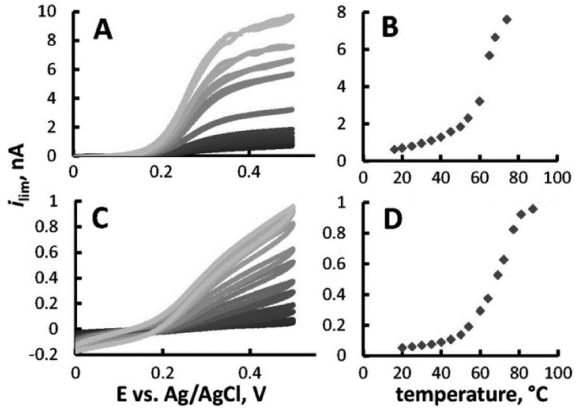

FIGURE 9. (A, C) Representative voltammetric responses and (B, D) plots of $Fc(CH_2OH)_2$ limiting current as a function of temperature for poly(L-alanine)–colloidal membrane Pt electrodes after polymerization for 1 and 3 h, respectively. Reproduced with permission from ref 43. Copyright 2009 Royal Society of Chemistry.

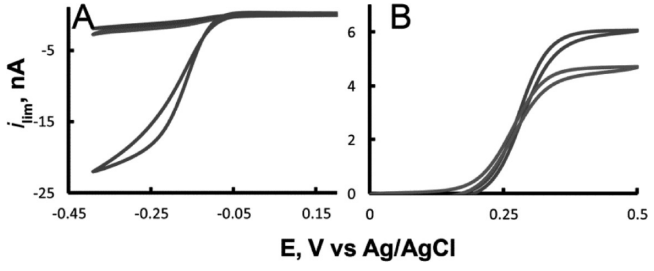

FIGURE 10. Representative voltammetric responses for PDMAEMA–colloidal film Pt electrodes (20 h polymerization) at different pH for $Ru(NH_3)_6^{3+}$ (A) and for $Fc(CH_2OH)_2$ (B). Voltammograms recorded above pH 5 are at the bottom in panel A and at the top in panel B. Voltammograms recorded below pH 4 are at the top in panel A and at the bottom in panel B. Reproduced with permission from ref 45. Copyright 2008 American Chemical Society.

increased at higher KCl concentration, which screened the charge on the polymer chains and thus facilitated the diffusion of $Ru(NH_3)_6^{3+}$. The diffusion of $Fc(CH_2OH)_2$ was not affected by ionic strength, suggesting that the conformation

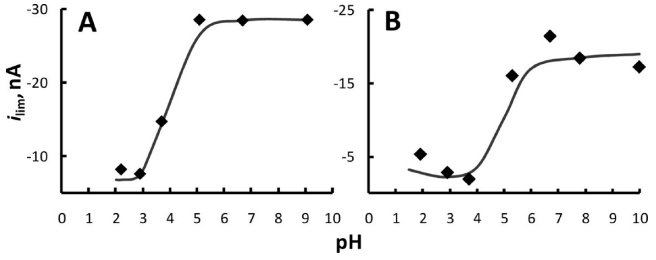

FIGURE 11. Limiting current ($Ru(NH_3)_6^{3+}$) as a function of increasing pH for PDMAEMA–colloidal membrane Pt electrodes for 5 h (A) and for 20 h (B) polymerizations. Reproduced with permission from ref 45. Copyright 2008 American Chemical Society.

of the PDMAEMA chains was not significantly affected by the charge screening under these conditions.

We also converted PDMAEMA into a polyelectrolyte brush with fixed charges by treating the polymer with ethyl bromide. The limiting current of both $Ru(NH_3)_6^{3+}$ and $Fc(CH_2OH)_2$ for the opal electrodes decreased significantly after the quaternization (Figure 12) and was not pH-dependent. Addition of 0.5 M KCl did not screen the positive charge of the quaternized polymer brush (Figure 12A), but small conformational changes in the polymer chains were evident from the limiting current change (Figure 12B).

Aptamer-Modified Colloidal Films[46]. To complete our studies of colloidal nanoporous films modified with responsive polymers, we explored a system where the polymer conformation responds to a small molecule binding. We used a responsive DNA aptamer[46] that exhibits selective and specific binding toward cocaine.[47] The secondary structure for this 32-base aptamer possesses a three-way junction, in the middle of which there is a cavity that binds the target molecule (Figure 13). In the absence of a target, the aptamer is thought to remain partially unfolded, with only one of the three junctions folded.

The aptamer described above was attached to the surface of silica colloidal film via maleimide-activated chemistry.

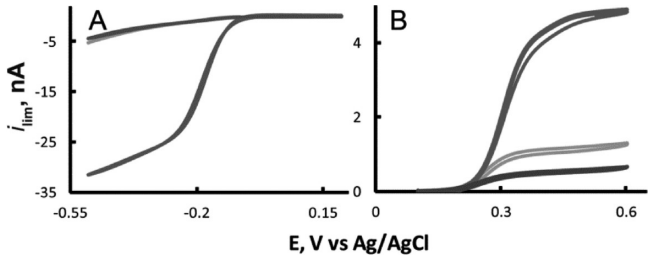

FIGURE 12. Representative voltammetric responses of PDMAEMA−colloidal film Pt electrodes for (A) $Ru(NH_3)_6^{3+}$ before quaternization (bottom), after quaternization (top), and after quaternization in the presence of 0.5 M KCl (top) and (B) $Fc(CH_2OH)_2$ before quaternization (top), after quaternization (bottom), and after quaternization in the presence of 0.5 M KCl (middle). Reproduced with permission from ref 45. Copyright 2008 American Chemical Society.

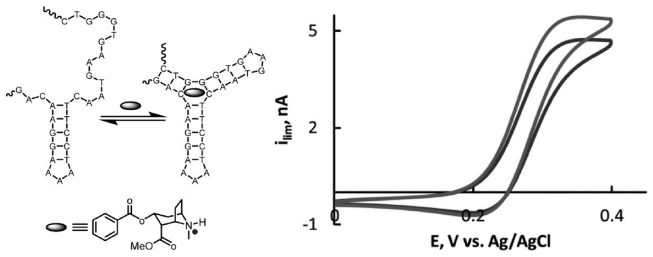

FIGURE 13. (left) Cocaine-sensing aptamer binding to cocaine and (right) representative $Fc(CH_2OH)_2$ voltammetric response for an aptamer-modified opal electrode in the absence (bottom) and in the presence of cocaine (top). Reproduced with permission from ref 46. Copyright 2011 Institute of Organic Chemistry and Biochemistry AS CR.

The flux of a redox-active probe molecule (ferrocene dimethanol) through the resulting nanoporous films was measured as a function of cocaine concentration using cyclic voltammetry. The limiting current for the aptamer-modified opal electrodes increased after the addition of cocaine to the solution (Figure 13). The observed reversible 9.0% ± 3.5% change corresponds to 0.6 nm increase in effective nanopore radius. This behavior was attributed to the conformational change as described above.

We found that the change in limiting current resulting from cocaine binding was affected by the size of the nanopore. For 7.8 nm "radius" nanopores, the limiting current increase was ca. 2.6 times higher compared with 22.5 nm nanopores. This observation was rationalized by assuming that the aptamer size change remains constant regardless of the nanopore size, thus having a greater effect for the smaller nanopores.

Free-Standing Silica Colloidal Membranes

Despite the fact that the silica colloidal films described above provide valuable fundamental information about the ionic and molecular transport through surface-modified inorganic nanopores, the practical applications of the films are limited. In order to prepare responsive colloidal membranes, free-standing structures were required. Our initial attempts to prepare free-standing membranes by suspending silica colloidal crystals in silicon[48] and glass[49] supports provided limited success. More recently, we discovered that mechanically durable and large area free-standing silica colloidal membranes[50] (Figures 14 and 15) can be prepared by physically bonding the colloidal spheres at 1050 °C. We confirmed that such membranes are crack-free and have no major defects by measuring their diffusional flux of $Fe(bpy)_3^{2+}$ in acetonitrile. Furthermore, we found that free-standing silica colloidal membranes show size selectivity for the diffusion of macromolecules.[51]

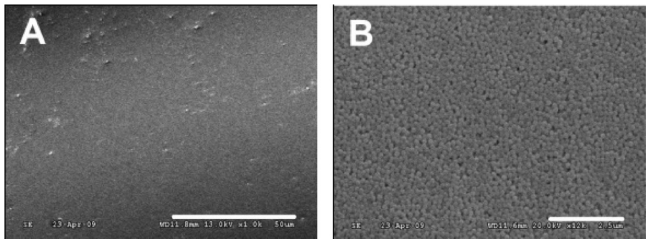

FIGURE 14. SEM images of sintered colloidal crystals comprised of 180 nm silica spheres: (A) SEM image showing no major cracks over a large area (size bar = 50 μm); (B) Magnified image displaying the close-packed fcc lattice (size bar = 2.5 μm). Reproduced with permission from ref 50. Copyright 2009 American Chemical Society.

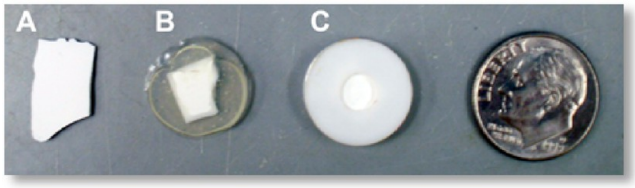

FIGURE 15. Photographs of sintered silica colloidal membranes: (A) as-sintered; (B) without PTFE washers showing the sintered colloidal membrane in the epoxy; (C) with PTFE washers. Reproduced with permission from ref 50. Copyright 2009 American Chemical Society.

Aminated Colloidal Membranes. In order to compare the electrostatic gating in free-standing colloidal membranes to that in thin colloidal films, we aminated the surface of the nanopores in free-standing membranes. This process required an additional rehydroxylation step because most of the surface hydroxyl groups are lost during the high temperature sintering used to prepare the free-standing membranes. Moreover, to introduce a relatively high number of amines onto the free-standing membrane surface, two treatments with 3-aminopropyltriethoxysilane were required.

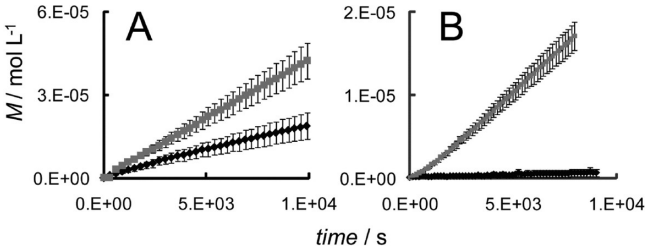

FIGURE 16. Diffusion rates of $Fe(bpy)_3^{2+}$ through PDMAEMA-modified colloidal membranes with (black) and without (gray) 50 mM trifluoroacetic acid after (A) 16 h and (B) 22 h of polymerization. Reproduced with permission from ref 52. Copyright 2010 Wiley, Inc.

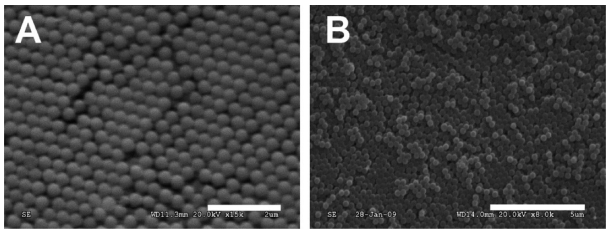

FIGURE 17. SEM images of (A) self-assembled and (B) sintered SiO_2@Au colloidal membranes. Scale bar is 2 μm in (A) and 5 μm in (B). Reproduced with permission from ref 53. Copyright 2013 American Chemical Society.

Even in this case, the amine coverage was 0.8 groups per nm^2, compared with 1.3 groups per nm^2 found for thin colloidal films. The twice-aminated free-standing membranes showed a modest electrostatic gating, with 22% decrease in the flux of $Fe(bpy)_3^{2+}$ under the acidic conditions. We explained this observation by the relatively small number of amine groups that could be placed on the surface of free-standing colloidal membranes.

PDMAEMA-Filled Colloidal Membranes[52]. In order to prepare free-standing colloidal membranes with pores filled with a responsive polymer, we formed PDMAEMA brushes on the surface of the colloidal nanopores. The silica surface was aminated, followed by the reaction with 2-bromoisobutyryl bromide and the by the ATRP of DMAEMA. The M_w of PDMAEMA after 16 h of polymerization was estimated as 20 kDa, after 22 h as 23 kDa, and after 44 h as 31 kDa. We demonstrated the reversible pH-responsive gating by the resulting membranes using diffusion measurements. We found that the flux of $Fe(bpy)_3^{2+}$ through the membranes modified with the polymer for 16 h decreased by 42% (2.4 times) when trifluoroacetic acid was added to solution (Figure 16A). Longer polymerization time (22 h) provided membranes with complete (95%) gating of $Fe(bpy)_3^{2+}$ flux (Figure 16B). We demonstrated that gating in these membranes can be tuned by polymer length, membrane thickness, and pore diameter and a complete acid-controlled gating can be achieved.

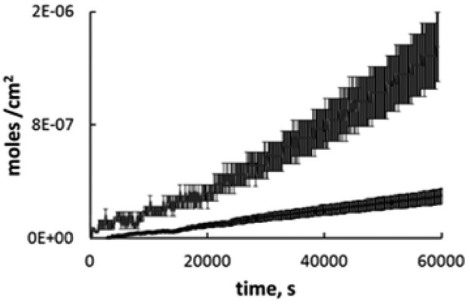

FIGURE 18. Representative plots of the molecular flux of ferrocene carboxaldehyde through the SiO_2@Au membranes modified with PMAA via ATRP for 45 min (with TFA, top; without TFA, bottom). Reproduced with permission from ref 53. Copyright 2013 American Chemical Society.

Free-Standing SiO_2@Au Colloidal Membranes

We prepared another type of gated colloidal membranes with different surface chemistry. Instead of using the silica spheres to assemble the membranes, we utilized gold-coated spheres.[53] Remarkably, the gold did not interfere with the self-assembly, and good quality colloidal crystals were formed (Figure 17A).[53] We were able to sinter these colloidal crystals to obtain free-standing membranes (Figure 17B), suitable for further surface modifications using thiol chemistry. We prepared electrostatically gated SiO_2@Au colloidal membranes by modifying the gold surface with L-cysteine, which allowed us to control the flux of a cationic dye by addition of acid. Furthermore, we prepared pore-filled SiO_2@Au colloidal membranes by surface-initiated polymerization of methacrylic acid (PMAA). We demonstrated over an order of magnitude increase of neutral dye flux through the PMAA-filled membranes upon addition of an acid, which results from the protonated polymer conformational change and increase in the free pore volume (Figure 18).

Summary and Outlook

In this Account, we described the preparation, surface modification, and transport properties of silica colloidal nanoporous films and membranes. They consist of colloidal spheres in close-packed fcc lattice with ordered arrays of interconnected nanopores. The films are formed by vertical deposition from colloidal solution onto various solid supports. They can also be suspended in a glass or silicon support. Free-standing colloidal membranes can be prepared by sintering

the self-assembled colloidal crystals above 1000 °C. The quality of the fcc packing in the membranes depends on the thickness of the crystal, with thinner films showing much better ordering. However, we showed that crystalline defects do not significantly affect the ionic and molecular flux through the membranes. Most importantly, in all cases the films and membranes can be prepared without mechanical defects.

We achieved surface modification of silica colloidal films and membranes using silanol chemistry and formed polymer brushes on the nanopore surface using atom transfer radical polymerization and ring-opening polymerization. The flux in the resulting nanoporous films and membranes has been be controlled by pH and ionic strength, temperature, light, and small molecule binding. We also showed that silica colloidal membranes possess size-selective diffusion of macromolecules.

Silica colloidal films and membranes described in this Account expand the growing family of responsive inorganic nanoporous materials.[54] There are various potential applications for silica colloidal membranes. Due to their ordered nanoporous structure and mechanical durability, they can be applied in nanofluidics, nanofiltration, separations,[55−60] sensing,[61,62] and fuel cells[63,64] and as catalyst supports. Reversible gating of flux in these membranes via external stimuli may be useful in drug-release devices, in size-, charge-, and structure-selective separations, and in microfluidic and sensing devices.

We thank all the group members and collaborators who have contributed to this research, as cited. We also acknowledge funding from NSF, ACS PRF, and CRDF.

BIOGRAPHICAL INFORMATION

Ilya Zharov is an Associate Professor of Chemistry at the University of Utah. He received B.S. and M.S. (Honors) degrees in 1990 from Chelyabinsk State University. He obtained his M.S. in 1994 from Technion-Israel Institute of Technology and Ph.D. in 2000 from the University of Colorado, Boulder. He was a Beckman Postdoctoral Fellow at University of Illinois, Urbana−Champaign and started his independent research and teaching career in Utah in 2003. He has received the Camille and Henry Dreyfus Foundation New Faculty Award and NSF CAREER Award among other recognitions and was named an Emerging Investigator by the Royal Society of Chemistry. Work in his group focuses on functional nanoporous materials.

Amir Khabibullin is a Ph.D. student working under the supervision of Professor Zharov. He was born in Russia and obtained his B.S. (Honors) in 2008 from Kazan State University. He was the winner of many National Chemistry Olympiads in Russia and received a Fulbright Fellowship to attend the graduate program at the University of Utah. His work focuses on porous materials for energy applications and on new types of nanoporous membranes.

FOOTNOTES

*Corresponding author. E-mail: i.zharov@utah.edu.
The authors declare no competing financial interest.

REFERENCES

1 Davis, M. E. Ordered Porous Materials for Emerging Applications. *Nature* **2002**, *417*, 813–821.
2 Bayley, H.; Martin, C. R. Resistive-Pulse Sensing-From Microbes to Molecules. *Chem. Rev.* **2000**, *100*, 2575–2594.
3 van Reis, R.; Zydney, A. Bioprocess Membrane Technology. *J. Membr. Sci.* **2007**, *297*, 16–50.
4 Afonso, C. A. M.; Crespo, J. G. Recent Advances in Chiral Resolution through Membrane-Based Approaches. *Angew. Chem., Int. Ed.* **2004**, *43*, 5293–5295.
5 Piruska, A.; Gong, M.; Sweedler, J. V.; Bohn, P. W. Nanofluidics in Chemical Analysis. *Chem. Soc. Rev.* **2010**, *39*, 1060–1072.
6 Orosz, K. E.; Gupta, S.; Hassink, M.; Abdel-Rahman, M.; Moldovan, L.; Davidorf, F. H.; Moldovan, N. I. Delivery of Antiangiogenic and Antioxidant Drugs of Ophthalmic Interest through a Nanoporous Inorganic Filter. *Mol. Vision* **2004**, *10*, 555–565.
7 Kipke, S.; Schmid, G. Nanoporous Alumina Membranes as Diffusion Controlling Systems. *Adv. Funct. Mater.* **2004**, *14*, 1184–1188.
8 Santini, J. T., Jr.; Cima, M. J.; Langer, R. A Controlled-Release Microchip. *Nature* **1999**, *397*, 335–338.
9 Nishizawa, M.; Menon, V. P.; Martin, C. R. Metal Nanotubule Membranes with Electrochemically Switchable Ion-Transport Selectivity. *Science* **1995**, *268*, 700–702.
10 Ito, T.; Sato, Y.; Yamaguchi, T.; Nakao, S. Response Mechanism of a Molecular Recognition Ion Gating Membrane. *Macromolecules* **2004**, *37*, 3407–3414.
11 Liu, G.; Lu, Z.; Duncan, S. Porous Membranes of Polysulfone-graft-poly(tert-butylacrylate) and Polysulfone-graft-poly(acrylic acid): Morphology, pH-Gated Water Flow, Size Selectivity, and Ion Selectivity. *Macromolecules* **2004**, *37*, 4218–4226.
12 Kallus, S.; Condre, J.-M.; Hahn, A.; Golemme, G.; Algieri, C.; Dieudonne, P.; Timmins, P.; Ramsay, J. D. F. Colloidal Zeolites and Zeolite Membranes. *J. Mater. Chem.* **2002**, *12*, 3343–3350.
13 Tong, H. D.; Jansen, H. V.; Gadgil, V. J.; Bostan, C. G.; Berenschot, C. G. E.; van Rijn, C. J. M.; Elwenspoek, M. Silicon Nitride Nanosieve Membrane. *Nano Lett.* **2004**, *4*, 283–287.
14 Striemer, C. C.; Thomas R. Gaborski, T. R.; McGrath, J. L.; Fauchet, P. M. Charge- and Size-Based Separation of Macromolecules Using Ultrathin Silicon Membranes. *Nature* **2007**, *445*, 749–753.
15 Yamaguchi, A.; Uejo, F.; Yoda, T.; Uchida, T.; Tanamura, Y.; Yamashita, T.; Teramae, N. Self-Assembly of a Silica-Surfactant Nanocomposite in a Porous Alumina Membrane. *Nat. Mater.* **2004**, *3*, 337–341.
16 Liu, N. G.; Dunphy, D. R.; Atanassov, P.; Bunge, S. D.; Chen, Z.; Lopez, G. P.; Boyle, T. J.; Brinker, C. J. Photoregulation of Mass Transport through a Photoresponsive Azobenzene-Modified Nanoporous Membrane. *Nano Lett.* **2004**, *4*, 551–554.
17 Hinds, B. J.; Chopra, N.; Rantell, T.; Andrews, R.; Gavalas, V.; Bachas, L. G. Aligned Multiwalled Carbon Nanotube Membranes. *Science* **2004**, *303*, 62–65.
18 Ulbricht, M. Advanced Functional Polymer Membranes. *Polymer* **2006**, *47*, 2217–2262.
19 Blanco, A.; Chomski, E.; Grabtchak, S.; Ibisate, M.; John, S.; Leonard, S. W.; Lopez, C.; Mesequer, F.; Miguez, H.; Mondia, J. P.; Ozin, G. A.; Toader, O.; Van Driel, H. M. Large-Scale Synthesis of a Silicon Photonic Crystal with a Complete Three-Dimensional Bandgap Near 1.5 Micrometres. *Nature* **2000**, *405*, 437–440.
20 Bartlett, P. N.; Ghanem, M. A.; Hallag, E.; De Groot, P.; Zhukov, A. Electrochemical Deposition of Macroporous Magnetic Networks Using Colloidal Templates. *J. Mater. Chem.* **2003**, *13*, 2596–2602.
21 Park, S. H.; Xia, Y. Macroporous Membranes with Highly Ordered and Three-Dimensionally Interconnected Spherical Pores. *Adv. Mater.* **1999**, *10*, 1045–1048.
22 Cassagneau, S.; Caruso, F. Semiconducting Polymer Inverse Opals Prepared by Electropolymerization. *Adv. Mater.* **2002**, *14*, 34–38.
23 Wong, S.; Kitaev, V.; Ozin, G. A. Colloidal Crystal Films: Advances in Universality and Perfection. *J. Am. Chem. Soc.* **2003**, *125*, 15589–15598.
24 Stoeber, W.; Fink, A.; Bohn, E. Controlled Growth of Monodisperse Silica Spheres in the Micron Size Range. *J. Colloid Interface Sci.* **1968**, *26*, 62–69.
25 Jiang, P.; Bertone, J. F.; Hwang, K. S.; Colvin, V. L. Single-Crystal Colloidal Multilayers of Controlled Thickness. *Chem. Mater.* **1999**, *11*, 2132–2140.
26 Onclin, S.; Ravoo, B. J.; Reinhoudt, D. N. Engineering Silicon Oxide Surfaces Using Self-Assembled Monolayers. *Angew. Chem., Int. Ed.* **2005**, *44*, 6282–6304.

27 Matyjaszewski, K.; Xia, J. Atom Transfer Radical Polymerization. *Chem. Rev.* **2001**, *101*, 2921–2990.

28 Cussler, E. L. *Diffusion, Mass Transfer in Fluid Systems*, 2nd ed.; Cambridge University Press: Cambridge, U.K., 1997.

29 Jiang, P.; Hwang, K. S.; Mittleman, D. M.; Bertone, J. F.; Colvin, V. L. *J. Am. Chem. Soc.* **1999**, *121*, 11630–11637.

30 Naegeli, R.; Redepenning, J.; Anson, F. C. Influence of Supporting Electrolyte Concentration and Composition on Formal Potentials and Entropies of Redox Couples Incorporated in Nafion Coatings on Electrodes. *J. Phys. Chem.* **1986**, *90*, 6227–6232.

31 Newton, M. R.; Bohaty, A. K.; White, H. S.; Zharov, I. Chemically Modified Opals as Thin Permselective Nanoporous Membranes. *J. Am. Chem. Soc.* **2005**, *127*, 7268–7269.

32 Newton, M. R.; Bohaty, A. K.; Zhang, Y.; White, H. S.; Zharov, I. pH and Ionic Strength Controlled Cation Permselectivity in Amine-Modified Nanoporous Opal Films. *Langmuir* **2006**, *22*, 4429–4432.

33 Smith, J. J.; Zharov, I. Ion Transport in Sulfonated Nanoporous Colloidal Films. *Langmuir* **2008**, *24*, 2650–2654.

34 Bohaty, A. K.; Newton, M. R.; Zharov, I. Light-Controlled Ion Transport Through Spiropyran-Modified Nanoporous Silica Colloidal Films. *J. Porous Mater.* **2010**, *17*, 465–473.

35 Cichelli, J.; Zharov, I. Chiral Selectivity in Surface-Modified Porous Colloidal Films. *J. Am. Chem. Soc.* **2006**, *128*, 8130–8131.

36 Lee, S. B.; Mitchell, D. T.; Trofin, L.; Nevanen, T. K.; Söderlund, H.; Martin, C. R. Antibody-Based Bio-Nanotube Membranes for Enantiomeric Drug Separations. *Science* **2002**, *296*, 2198–2201.

37 Rmaile, H. H.; Schlenoff, J. B. Optically Active Polyelectrolyte Multilayers as Membranes for Chiral Separations. *J. Am. Chem. Soc.* **2003**, *125*, 6602–6603.

38 Mollard, A.; Ibragimova, D.; Antipin, I. S.; Stoikov, I. I.; Zharov, I. Molecular Transport in Thiacalixarene-Modified Nanoporous Colloidal Films. *Microporous Mesoporous Mater.* **2010**, *131*, 378–384.

39 Cichelli, J.; Zharov, I. Chiral Permselectivity in Nanoporous Opal Films Surface-Modified with Chiral Selector Moieties. *J. Mater. Chem.* **2007**, *17*, 1870–1875.

40 Schepelina, O.; Zharov, I. PNIPAAM-Modified Nanoporous Colloidal Films with Positive and Negative Temperature Gating. *Langmuir* **2007**, *23*, 12704–12709.

41 Heskins, M.; Guillet, J. E. Solution Properties of Poly(N-isopropylacrylamide). *J. Macromol. Sci., Chem.* **1968**, *2*, 1441–1455.

42 Schepelina, O.; Zharov, I. Polymer-Modified Opal Nanopores. *Langmuir* **2006**, *22*, 10523–10527.

43 Abelow, A. E.; Zharov, I. Poly(L-alanine)-Modified Nanoporous Colloidal Films. *Soft Matter* **2009**, *5*, 457–462.

44 Mart, R. J.; Osborne, R. D.; Stevens, M. M.; Ulijn, R. V. Peptide-Based Stimuli-Responsive Biomaterials. *Soft Matter* **2006**, *2*, 822–835.

45 Schepelina, O.; Zharov, I. Poly(2-(dimethylamino)ethyl methacrylate)-Modified Nanoporous Colloidal Films with pH and Ion Response. *Langmuir* **2008**, *24*, 14188–14194.

46 Abelow, A. E.; White, R. J.; Plaxco, K. W.; Zharov, I. Nanoporous Silica Colloidal Films with Molecular Transport Gated by Aptamers Responsive to Small Molecules. *Collect. Czech. Chem. Commun.* **2011**, *76*, 683–694.

47 Stojanovic, M. N.; Prada, P.; Landry, D. W. Aptamer-Based Folding Fluorescent Sensor for Cocaine. *J. Am. Chem. Soc.* **2001**, *123*, 4928–4931.

48 Bohaty, A. K.; Zharov, I. Suspended Self-Assembled Opal Membranes. *Langmuir* **2006**, *22*, 5533–5536.

49 Bohaty, A.; Abelow, A. E.; Zharov, I. Nanoporous Silica Colloidal Membranes Suspended in Glass. *J. Porous Mater.* **2011**, *18*, 297–304.

50 Bohaty, A. K.; Smith, J. J.; Zharov, I. Free-Standing Silica Colloidal Nanoporous Membranes. *Langmuir* **2009**, *25*, 3096–3101.

51 Ignacio-de Leon, P. A.; Zharov, I. Size-Selective Transport in Colloidal Nano-Frits. *Chem. Commun.* **2011**, *47*, 553–555.

52 Schepelina, O.; Poth, N.; Zharov, I. pH-Responsive Nanoporous Silica Colloidal Membranes. *Adv. Funct. Mater.* **2010**, *20*, 1962–1969.

53 Ignacio-de Leon, P. A.; Zharov, I. SiO_2@Au Core-Shell Nanospheres Self-Assemble To Form Colloidal Crystals That Can Be Sintered and Surface Modified To Produce pH-Controlled Membranes. *Langmuir* **2013**, *29*, 3749–3756.

54 Abelow, A. E.; Zharov, I. Reversible Nanovalves in Inorganic Materials. *J. Mater. Chem.* **2012**, *22*, 21810–21818.

55 Zhang, H.; Wirth, M. J. Electromigration of Single Molecules of DNA in a Crystalline Array of 300 nm Silica Colloids. *Anal. Chem.* **2005**, *77*, 1237–1242.

56 Zheng, S.; Ross, E.; Legg, M. A.; Wirth, M. J. High-Speed Electroseparations inside Silica Colloidal Crystals. *J. Am. Chem. Soc.* **2006**, *128*, 9016–9017.

57 Wei, B.; Malkin, D. S.; Wirth, M. J. Plate Heights below 50 nm for Protein Electrochromatography Using Silica Colloidal Crystals. *Anal. Chem.* **2010**, *82*, 10216–10221.

58 Wei, B.; Rogers, B.; Wirth, M. J. Slip Flow in Silica Colloidal Crystals for Ultra-Efficient Chromatography. *J. Am. Chem. Soc.* **2012**, *134*, 10780–10782.

59 Rogers, B.; Wirth, M. J. Slip Flow through Hydrophobic Silica Colloidal Crystals of Varying Particle Diameter. *ACS Nano* **2013**, *7*, 725–731.

60 Njoya, N. K.; Birdsall, R. E.; Wirth, M. J. Silica Colloidal Crystals as Emerging Materials for High-Throughput Protein Electrophoresis. *AAPS J.* **2013**, *15*, 962–969.

61 Zheng, S.; Zhang, H.; Ross, E.; Le, T. V.; Wirth, M. J. Silica Colloidal Crystals for Enhanced Fluorescence Detection in Microarrays. *Anal. Chem.* **2007**, *79*, 3867–3872.

62 Velarde, T. R. C.; Wirth, M. J. Silica Colloidal Crystals as Porous Substrates for Total Internal Reflection Fluorescence Microscopy of Live Cells. *Appl. Spectrosc.* **2008**, *62*, 611–616.

63 Smith, J. J.; Abbaraju, R. R.; Zharov, I. Proton Transport in Assemblies of Silica Colloidal Spheres. *J. Mater. Chem.* **2008**, *18*, 5335–5338.

64 Smith, J. J.; Zharov, I. Preparation and Proton Conductivity of Self-Assembled Sulfonated Polymer-Modified Silica Colloidal Crystals. *Chem. Mater.* **2009**, *21*, 2013–2019.